Laminar Dispersion in Capillaries: Part II.

Effect of Inlet Boundary Conditions and Turner Type of System Capacitance

WILLIAM N. GILL

Clarkson College of Technology, Potsdam, New York

V. ANANTHAKRISHNAN

Syracuse University, Syracuse, New York

The effect of inlet boundary conditions on the transient approach to the asymptotic Taylor-Aris theory was studied for three different cases. It was found that for values of τ of practical interest the solutions for these cases were different only if $N_{Pe} < 100$. The asymptotic solution was independent of inlet conditions in the three cases studied once τ exceeded the necessary minima.

A rather complete numerical solution to the equation that describes laminar flow in tubes with a single continuous stagnant pocket of arbitrary depth along the entire length of the pore has been obtained, and results for point, average, and bulk concentration distributions are presented for a wide range of parameters. The range of applicability is extended to infinity for both τ and N_{Pe} by the asymptotic theory of Aris.

Higher capacitance systems require longer times before their dispersion behavior can be described by error-function solutions. This is important, since only then is the concept of an equivalent axial dispersion coefficient useful because then it allows the calculation of the complete average concentration distribution from a minimum of data. This suggests that in work on high capacitance systems such as packed beds, one should ensure that experimental systems are long enough for the asymptotic theory to apply if results are to be interpreted in terms of dispersion coefficients.

Numerical results for the Turner model agree very well with the modified effective dispersion coefficient, which was suggested by Aris and is given in Equation (15), as long as τ is sufficiently large. These lower limits for τ are given in Table 3. When the lower limits on τ are exceeded, the new solution developed for the point distribution given by Equations (31) and (32) is also valid. This is important for at least two reasons. First, it implies that the dispersion model can be used to describe the local as well as the average behavior of complex transient systems if only the velocity distribution across the system is known. More work is needed to ascertain the limitations and possibilities of the dispersion model in this regard. Second, it shows that one can find simple and accurate approximate local solutions without neglecting axial molecular diffusion.

In Part I* of this series (*1*) unsteady laminar miscible dispersion in simple capillaries was studied for a step change in concentration at the inlet boundary. It was shown, with natural convection assumed to be negligible, that the Taylor-Aris theory is valid when the single restriction of sufficiently large dimensionless time τ is met. The present paper extends previous results to include the effects of various inlet boundary conditions and of system capacitance. Part III will describe a comprehensive experimental program on dispersion in horizontal tubes.

Porous media consist of extremely small and geometrically complex capillaries of various lengths which are distributed in a more or less random fashion. A theoretical analysis which would consider all of the factors that affect mass transfer in a porous medium is almost impossible to develop with the present state of knowledge. Therefore, to analyze theoretically the complex phenomenon of miscible dispersion, many investigators emphasized a few specific effects and worked on physical or mathematical models which neglected or minimized other effects. Since the elementary mechanisms which constitute the overall dispersion process are assumed to be described by linear laws, it follows that each of these mechanisms can be studied independently and then the overall process can be described by the superposition of the individual elementary effects.

A model which describes one elementary mechanism, the capacitance effect, has been suggested by Turner (*9*). This model emphasizes the large capacitance effects present in porous media due to the existence of torturous bends and dead-end spaces along the flow paths. Turner pictures the porous medium as consisting of main channels of pores which have a uniform cross-sectional shape and area, through which the fluid flows. Communicating with the main channel are dead-end stagnant pockets which are distributed uniformly along the length of the

V. Ananthakrishnan is at Clarkson College, Potsdam, New York.

* The right-hand side of Equation (47) in Part I should be zero. Thus the paragraph of discussion on page 1070 related to Equation (51) is not relevant to the dispersion problem and should be disregarded.

pores. There is no bulk flow in or out of these pockets and the only mechanism for mass transfer in these pockets is molecular diffusion. However, in the main channel mass transfer is due to both diffusion and convection.

This model, assumed to be a reasonably adequate representation of at least one of the main effects occurring in actual porous media, provides a simple physical picture of the geometry involved, which reduces to an ordinary tube when the capacitance is zero. But even with this simplified model, the mathematics which results when one attempts to describe the diffusional phenomena in detail can still be quite complicated.

Turner assumed an effective Taylor diffusion coefficient and derived equations which described the response of this model to a sinusoidal concentration input. He made no attempt to justify these equations as related to the equations of change, but showed that they could be used with experimental data to determine the distribution of volumes and depths of pockets. In this way he characterized the flow structure by determining the residence time distribution for flow in porous media.

In a later paper Turner (*10*) described experiments in which he measured the response of a physical model to a sinusoidal concentration input. With these data and the equations from his previous analysis, he was able to calculate the ratio of stagnant pocket volume to channel volume. The ratio of these volumes calculated from the experimental concentration–time data agreed reasonably well with the actual volume ratio in his apparatus.

Aris (*3*) generalized Turner's model by allowing the stagnant pockets to have all possible depths. He also showed how the mass transfer in this medium could be affected by the distribution of pockets. In a later paper, by considering the diffusional structure, Aris (*4, 5*) showed that Turner's assumption regarding the magnitude of the effective Taylor diffusion coefficient needed to be modified. He indicated that actual values of the coefficient could be anywhere from one to eleven times the value that Turner used. The low value occurs when there are no pockets and the high value occurs when the ratio of the pocket volume to pore volume becomes infinite. Actually, the upperbound depends on geometry, and if the pockets are concentric annuli the ratio of dispersion coefficients is unbounded; that is, $\alpha \rightarrow \infty$.

The extent to which inlet boundary conditions influence transient dispersion problems in general has not yet been established. If it is to be of practical value, the Taylor-Aris theory, which is asymptotic for large τ, must be independent of the inlet boundary condition. It appears that this is not universally the case, since Philip's study (*7*) of the steady state periodic problem indicates that periodic systems are characterized by a complex dispersion coefficient. Consequently, the present study will investigate several aperiodic boundary conditions which are significantly different from each other and will determine how large τ must be for the Taylor-Aris theory to apply.

One seemingly useful method of classifying a dispersion system is according to the nature of the asymptotic solution for large values of time associated with it. In this context, three different classes of systems seem to exist:

1. Systems characterized by steady state, time-independent, asymptotic solutions which are generated by internal source or sink effects or by externally supported interphase transport.
2. Steady state periodic solutions which reflect the nature of the input forcing function.
3. Taylor types of solutions which are generated physically only by internal diffusion and convection processes. Asymptotic solutions for this class of problems appear to be much newer than those in classes 1 and 2.

The present work considers Turner's model, and the purposes of this work are

1. To investigate the importance of the inlet boundary condition used in posing the dispersion problem insofar as it affects: (a) local mass transfer in capillary flows during the dimensionless time interval before the diffusion model is valid, and (b) the magnitude of τ necessary for the Taylor-Aris theory to apply in capillary flows,
2. To analyze the effect of system capacitance in the sense of 1a and 1b.
3. To study the effect of Peclet number on the local behavior of systems with various inlet boundary conditions and with Turner type of capacitance,
4. To study the influence of system capacitance on the dispersion coefficient to establish quantitative criteria for the accuracy of Aris' theory of Turner structures,
5. To extend the Taylor-Aris theory to Turner types of systems by determining and testing new solutions to the diffusion equation for point concentrations and to specify the magnitudes of τ above which the solutions are valid.

MATHEMATICAL DESCRIPTION OF THE MODEL

A schematic representation of the Turner model is given in Figure 1*a*. This problem appears to consist of two regions; thus it is the usual practice to write continuity equations for both the main channel and the pockets and then to solve these two differential equations simultaneously by using the boundary conditions at the interface between the moving and stagnant fluids. This approach is complicated, but a significant simplification results if one recognizes that the main channel and pores can be considered a single region if the velocity distribution is chosen properly. Then one can analyze the problem by using an approach similar to that employed by the authors in Part I of this series.

In order to simplify this model slightly, it was decided to use a single continuous stagnant pocket of arbitrary depth along the entire length of the pore. Figure 1*b* illustrates this system schematically. This was done only for convenience, since the finite-difference method used to solve this system can also be used to solve the Turner model with a series of stagnant pockts of varying cross sections and various depths along the length of the pore. However this involves more parameters and is therefore more tedious. Furthermore, the continuous pocket model is sufficient to establish reasonably general criteria for the validity of Aris' theory.

The differential equation and the boundary conditions describing this system are given as

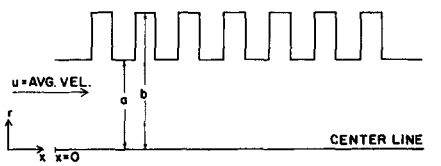

Fig. 1*a*. Schematic diagram of Turner's model.

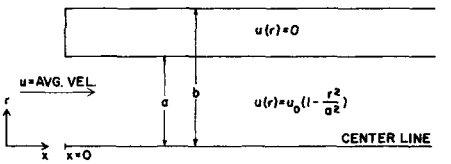

Fig. 1*b*. Schematic diagram of Turner's model with continuous stagnant pocket.

$$D\left(\frac{\partial^2 C^+}{\partial x^2}+\frac{\partial^2 C^+}{\partial r^2}+\frac{1}{r}\frac{\partial C^+}{\partial r}\right)=\frac{\partial C^+}{\partial t}+u\frac{\partial C^+}{\partial x} \tag{1}$$

and the velocity u is given as

$$\begin{aligned} u &= u_o\left(1-\frac{r^2}{a^2}\right) \qquad 0\le r\le a \\ &= 0 \qquad\qquad\qquad a\le r\le b \end{aligned} \tag{2}$$

The boundary and initial conditions are

$$\left.\begin{aligned} &C^+(0,x,r)=0, \quad x>0 \\ &C^+(t,-\infty,r)=C^+_\infty(t,r), \quad 0\le r\le a \\ &\frac{\partial C^+}{\partial x}(t,0,r)=0, \quad a\le r\le b \\ &C^+(t,\infty,r)=0 \\ &\frac{\partial C^+}{\partial r}(t,x,0)=0 \\ &\frac{\partial C^+}{\partial r}(t,x,b)=0 \end{aligned}\right\} \tag{3}$$

The condition $\frac{\partial C^+}{\partial x}(t,0,r)=0$, for $a\le r\le b$ is used, since it is assumed that material can enter or leave the system only in the region where a finite velocity exists.

In order to make this system dimensionless, the following transformations can be used:

$$\begin{aligned} X &= \frac{x}{N_{Pe}a};\quad N_{Pe}=\frac{au_o}{D};\quad \tau=\frac{tu_o}{aN_{Pe}} \\ \eta &= \frac{X}{\sqrt{\tau}};\quad y=\frac{r}{a};\quad C=\frac{C^+}{C^+_\infty} \end{aligned} \tag{4}$$

By introducing these transformations, if C^+_∞ is a constant, the system reduces to

$$\frac{\partial C}{\partial \tau}+\left[\frac{u(y)}{\sqrt{\tau}}-\frac{1}{2}\frac{\eta}{\tau}\right]\frac{\partial C}{\partial \eta} = \frac{\partial^2 C}{\partial y^2}+\frac{1}{y}\frac{\partial C}{\partial y}+\frac{1}{\tau N_{Pe}^2}\frac{\partial^2 C}{\partial \eta^2} \tag{5}$$

with the conditions

$$\begin{aligned} &C(0,\eta,y)=0 \quad \eta>0 \\ &C(\tau,-\infty,y)=1, \quad 0\le y\le 1; \quad \frac{\partial C}{\partial \eta}(\tau,0,y)=0, \\ &\qquad\qquad 1\le y\le \frac{b}{a} \\ &C(\tau,\infty,y)=0 \\ &\frac{\partial C}{\partial y}\left(\tau,\eta,\frac{b}{a}\right)=0 \\ &\frac{\partial C}{\partial y}(\tau,\eta,0)=0 \end{aligned} \tag{6}$$

This system applies for all y's where

$$\begin{aligned} u(y) &= 1-y^2 \quad 0\le y\le 1 \\ u(y) &= 0 \qquad\quad 1\le y\le \rho \end{aligned} \tag{7}$$

and

$$\rho = b/a$$

To determine the importance of inlet boundary conditions, the following cases were investigated:

A. Step change in inlet concentration for $\tau>0$, $C(\tau,0,y)=1$. This condition applies best to situations where the feed section supplied material to the inlet as a well-mixed tank would do.

B. $C(\tau,-\infty,y)=1$. This condition is exact where, say, two identical infinitely long capillaries, one with unit and the other with zero concentration, are initially separated by a partition. Then flow is started and the partition is removed simultaneously.

C. As an approximation to case B, one can employ Danckwerts' boundary condition at the inlet as

$$D\frac{\partial C^+}{\partial x}+u(C^+_\infty-C^+)=0 \quad \text{at} \quad x=0$$

which, when put in dimensionless form, results in

$$\frac{1}{\sqrt{\tau}\,N_{Pe}^2}\frac{\partial C}{\partial \eta}(\tau,0,y)+(1-y^2)(1-C)=0 \tag{8}$$

Wehner and Wilhelm (9) discussed the applicability of this inlet condition for steady state systems.

System A has been discussed in detail for tubes in Part I of this series and requires fairly minor changes for Turner's model. Systems B and C are treated in similar fashion but the condition at the entrance varies with time. In case B the finite-difference solution is carried out by having initially a block of unit concentration up to the entrance and the remaining portion of the system is kept at zero concentration. This is shown in Figure 2. Computations are then carried out in the usual manner for the entire tube starting from $x=-a$. The concentration at $x=-a$ is fixed at unity in all the calculations. When back diffusion causes the concentration near $x=-a$ to change so that the condition of $C=1.0$ at $x=-a$ is no longer valid, the region of unit concentration is extended backward from the entrance and the procedure is repeated. In this manner concentration distributions were obtained for rather wide ranges of N_{Pe} and τ.

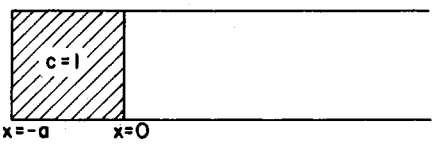

Fig. 2. Illustration of inlet boundary condition for case B.

The treatment of case C is exactly the same as A, except for the condition at $x=0$. Details of the finite-difference method for solving case A were given previously (1) and extension to cases B and C is rather straightforward.

DISCUSSION OF RESULTS FOR DIFFERENT ENTRANCE CONDITIONS IN A CAPILLARY TUBE MODEL

Complete sets of results have been obtained here for both cases B and C for various Peclet numbers, and results for case A are available from Part I. Four Peclet numbers were studied to determine the magnitude of differences in the concentration distributions obtained with the three different cases and to establish whether all systems behave in an identical manner asymptotically. Peclet numbers >

1,000 were used for the high N_{Pe} region, while in the lower region, $N_{Pe} = 25$, 10, and 1 were studied.

Figure 3 is a plot of average concentration of the solute as a function of dimensionless axial distance X/τ for $\tau = 0.006$. It is clear that even at this very low value of τ all three inlet conditions give the same average concentration distribution. This obviously should occur since at high Peclet numbers, Equation (8) reduces to the step change condition. Since the results are identical at $\tau = 0.006$, they also will be the same at higher τ values and it can be concluded that for the high Peclet number region the solution to the dispersion equation is independent of the entrance conditions used, at all times of practical interest. Figures 4 and 5 represent the average concentration distribution plots, for a Peclet number of 10, where the effect of axial molecular diffusion is significant as was found to be true for all $N_{Pe} < 100$. Similar data have been computed for $N_{Pe} = 25$, 1.*

It can be seen from these results that the distributions obtained from the three inlet conditions are quite different at lower values of τ. However, as τ increases the three solutions eventually become identical. For Peclet numbers of 25 and 10 the limiting values of τ above which the concentration distributions are independent of the entrance condition are approximately equal to $\tau = 0.600$, 1.750. Solutions with the use of conditions B and C, become identical at smaller τ as one would expect, since they are identical conditions in the steady state case. For several N_{Pe} Table 1 compares the limiting τ values above which the concentration distributions for the various inlet conditions are the same.

From the results obtained it can be seen that the solutions are more sensitive to inlet conditions at lower Peclet numbers and lower values of τ. It is known that for sufficiently short times, axial molecular diffusion predominates over convection, and this can be seen in Figures 4 and 5 from the fact that solute extends beyond $X/\tau = 1.0$. As dimensionless time increases, dispersion by convection becomes more significant and at a sufficiently large τ, regardless of N_{Pe}, the two mechanisms create the dispersion in accordance with Aris' theory. This is seen in Figure 5, where the distance, in terms of X/τ at which solute exists, attenuates with increasing τ. It is interesting to note that in all cases investigated, after sufficient time has elapsed for the solute to be contained in the region $1 \geqq X/\tau$, the solutions for cases A, B, and C are, for practical purposes, identical. An estimate of the value of time, τ, necessary for this to occur, for $N_{Pe} \leqq 25$, can be obtained from Table 1. The results for N_{Pe} also can be viewed as corresponding to the pure diffusion case with a convective perturbation.

A significantly different property of case B solutions at low N_{Pe} is that they pass through the point ($X/\tau = 0.5$, $C_m = 0.5$) and are nearly straight lines on probability plots at much smaller dimensionless times than the other cases. This behavior is important since it decreases the values of τ necessary for the Taylor-Aris theory to be valid and therefore extends the range of applicability of

* Several additional figures of plotted data have been deposited as document 8997 with the American Documentation Institute, Photoduplication Service, Library of Congress, Washington 25, D. C., and may be obtained for $10.00 for photoprints or $3.50 for 35-mm. microfilm.

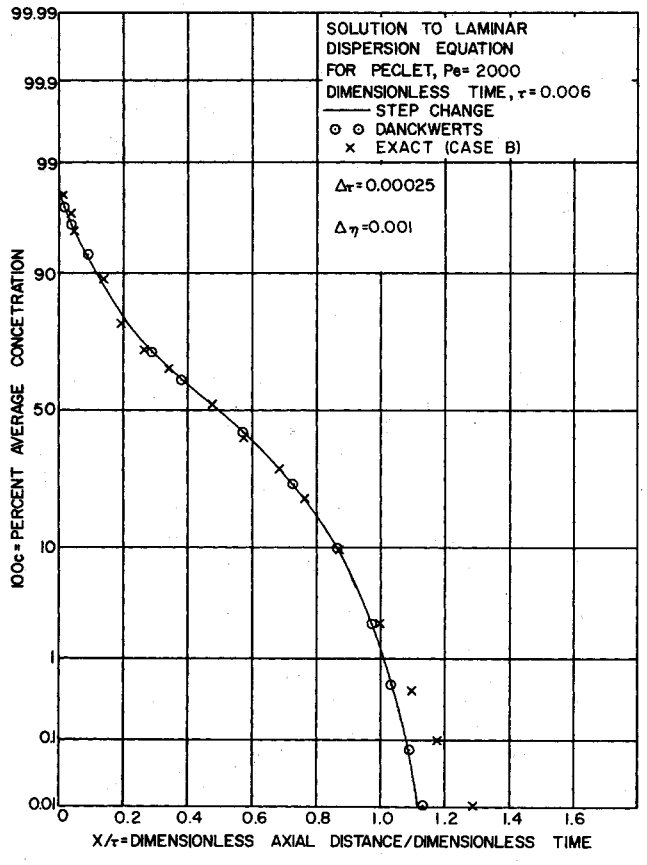

Fig. 3. Comparison of numerical results for different entrance conditions for $N_{Pe} = 2{,}000$ and $\rho = 1.0$.

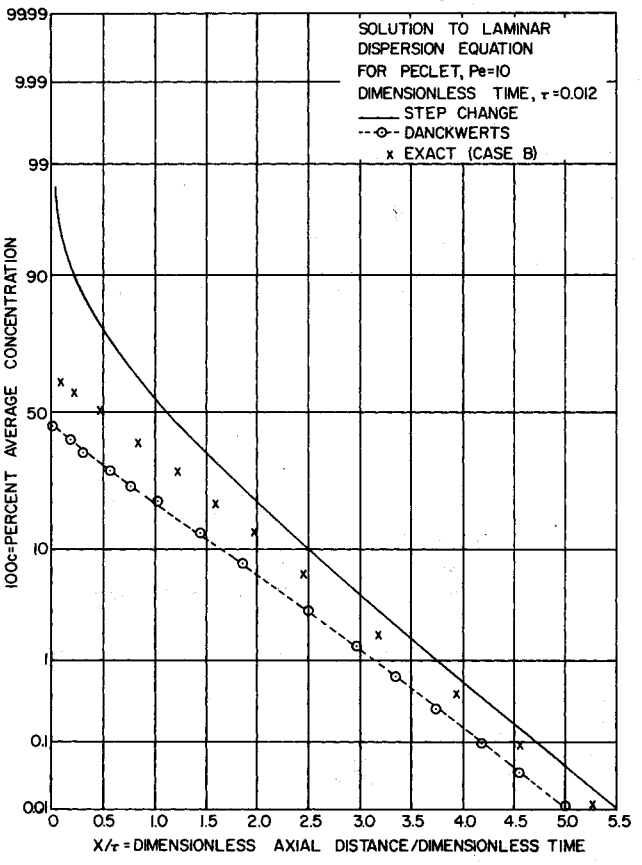

Fig. 4. Comparison of numerical results for different entrance conditions with $N_{Pe} = 10$ and $\rho = 1.0$.

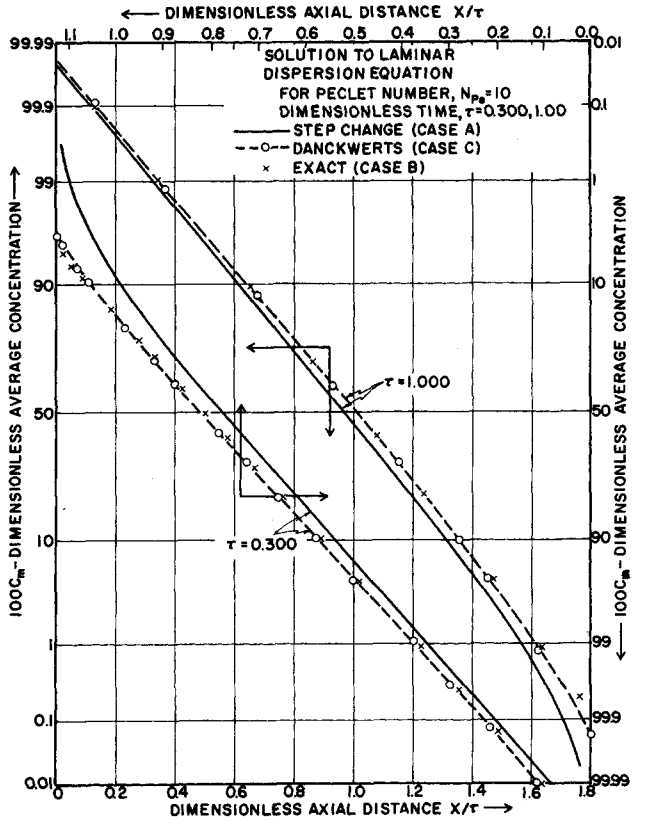

Fig. 5. Comparison of numerical results for different entrance conditions with N_{Pe} number = 10, the ratio of the radii ρ = 1.0, and for dimensionless times τ = 0.300 and 1.000. Note that results of cases B and C agree with each other for both τ used, whereas case A differs in each case.

the dispersion model. For example, the results in Table 1 show for N_{Pe} = 10 and 1 that case B requires minimum dimensionless times of about 0.5 and 4.5, and in case A 1.75 and > 20, respectively. This implies that experiments at low N_{Pe} can be affected by inlet conditions, which may be particularly important in high capacitance porous media as will be discussed later in conjunction with Turner model results.

TABLE 1. CAPILLARY MODEL

ρ = 1.0; approximate τ values above which:
(i) solution follows Aris' modification for case A
(ii) solutions for cases B and C are same
(iii) solutions for cases A, B, and C are same
(iv) solution for case B follows Aris' modification

N_{Pe}	τ_{min} for (i)	τ_{min} for (ii)	τ_{min} for (iii)	τ_{min} for (iv)
1,000	0.800	0.0	0.0	0.800
25	1.25	0.050	0.600	1.250
10	1.75	0.400	1.750	0.500
1	>20.0	>4.500	>4.500	about 4.500

TURNER MODEL RESULTS

The analysis of the Turner model problem described by Equations (5), (6), and (7) uses a modified version of the same technique described in Part I of this series (*1*). The main difference lies in the fact that, instead of having the parabolic velocity profile throughout the entire tube, it now exists only in the main channel while in the stagnant phase, the velocity is zero. Second, instead of applying over the entire radius, the entrance conditions A, B, and C, now apply only in the main channel, while in the capacitance section a zero axial gradient condition is appropriate. Details of the Peaceman-Rachford (*6*) finite-difference method of solving this system are reported elsewhere.*

The problem posed here for Turner systems involves three independent variables (τ, η, y) and three parameters (ρ, N_{Pe}, IBC), if one includes the effect of different inlet boundary conditions (IBC). Since the complete determination of solutions for a single set of values of the parameters involves considerable computation, it is clear that the computation job would be horrendous unless one limits markedly both the number of combinations of parameter values and the magnitudes of the independent variables studied. Thus it is of great importance that the solutions are identical for all high N_{Pe}, and that Aris' theory extends the results to infinite τ.

Solutions have been obtained for different main channel inlet conditions, cases A, B, and C for all combinations of the other parameters studied, and detailed results have been computed for Peclet numbers equal to 1,000, 25, 10, and 1.† In order to determine when the effect of axial diffusion is significant, concentration distributions have been obtained for very small τ for N_{Pe} = 500, 100, 75, and 50. It was found for values of τ of practical interest that axial molecular diffusion contributes negligibly for N_{Pe} > 100 and that the solutions are identical to those of N_{Pe} = 1,000. However, axial diffusion does become very significant as the Peclet number decreases from 100 to 1.

In order to study the effect of the ratio of main channel to stagnant phase volume on the dispersion process complete sets of results have been obtained at a high Peclet number of 1,000 for values of the ratio, b/a = ρ, equal 1.0, 1.1, 1.2, 1.3, 2.0.† It is worthwhile to note at this point that ρ = 1.0 is simply the Taylor problem (tube flow with no capacitance). However, low Peclet number results have been obtained only for ρ = 1.0, 1.2, since this serves to illustrate adequately the N_{Pe} effect in systems with capacitance.

The High Peclet Number Region

First, the high N_{Pe} region for Turner types of systems will be considered and the concentration distribution valid for all values of τ will be discussed. As in the case of the Taylor problem, it was found that concentration distributions are independent of entrance conditions for high Peclet numbers. Figures 6 and 7 represent plots of average concentration of solute over the entire tube, including the stagnant region, as a function of dimensionless axial distance X/τ for various τ values and N_{Pe} = 1,000. In each figure data are plotted for the four values of ρ investigated along with ρ = 1.0, for comparison.

At short times, say, τ = 0.006, dispersion in the main channel takes place by pure convection only. This was found by plotting on a linear scale the curve of C_m vs. X/τ as a straight line, which is the pure convection solution $(1 - X/\tau)$. At higher times radial dispersion be-

* The details of the mathematical analysis are available elsewhere. See footnote on page 909.

† All the numerical results obtained have been tabulated in terms of average and bulk concentration distribution for the entire range of τ and N_{Pe} and are available elsewhere. See footnote on page 909.

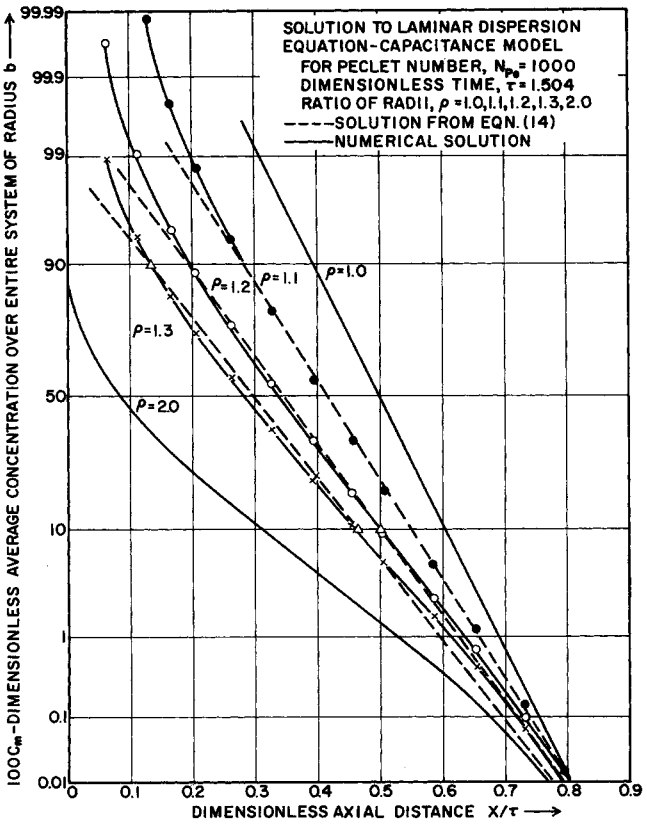

Fig. 6. Comparison of numerical results for different volume ratios in capacitance model with N_{Pe} = 1,000 and dimensionless time τ = 1.504.

comes more important and more solute starts to diffuse into the stagnant liquid. The curves are no longer symmetrical with respect to the pure convection solution as in the case of $\rho = 1.0$.

At sufficiently large times, the solutions become error functions as evidenced by their linearity on probability graphs in Figures 6 and 7. Again, one sees from these figures that at lower values of ρ, the solution becomes an error function faster. In other words, high capacitance systems require longer times before the behavior of the system can be described by the Taylor-Aris dispersion model. This result may have considerable significance regarding the description of dispersion in porous media.

It is known that for the Taylor problem (8) with high N_{Pe} and $\rho = 1.0$, the approximate analytical solution for the high τ value range is given by

$$C_m = 0.5 \text{ erfc} \left[\frac{(x - u_o t/2)}{\sqrt{4kt}} \right] \tag{9}$$

where

$$k = \frac{a^2 u_o^2}{192\, D} \tag{10}$$

In the present study it was deduced that for $\rho > 1$, Equation (9) remains valid if $u_o \rightarrow u_o/\rho^2$ and $a \rightarrow \rho a$, such that Equation (9) becomes

$$C_m = 0.5 \text{ erfc} \left[\frac{x - u_o t/2\rho^2}{\sqrt{4\, kt/\rho^2}} \right] \tag{11}$$

Furthermore, Aris (4) has shown that the effective Taylor diffusion coefficient has to be corrected for the presence of stagnant pockets; thus one obtains

$$k = \left[\frac{8(1+\beta) + 12\,(1+\beta)^2 \ln (1+\beta) - 7\,(1+\beta)^2}{(1+\beta)^2} \right] \frac{u_o^2\, a^2}{192\, D} \tag{12}$$

where

$$\beta = \rho^2 - 1 \tag{13}$$

The result of significance here is the occurrence of ρ in Equation (11) in order for Equation (12) to be valid.

It can be seen clearly from Equation (12) that for $\rho = 1.0$, $\beta = 0$, and hence k reduces to the effective Taylor diffusion coefficient given by Equation (10). By transforming to dimensionless form, Equation (11) becomes

$$C_m = 0.5 \text{ erfc} \left[\frac{X - (\tau/2\,\rho^2)}{\sqrt{\alpha\, \tau/48\rho^2}} \right] \tag{14}$$

where

$$\alpha = \frac{8(1+\beta) + 12\,(1+\beta)^2 \ln (1+\beta) - 7\,(1+\beta)^2}{(1+\beta)^2} \tag{15}$$

Equations (11) and (14) show that the dispersion in Turner structures must be considered to take place in a tube of radius b rather than a; then Equation (12) is the proper expression for the dispersion coefficient. This suggests that for complex systems the entire void volume, including any stagnant regions, should be used in determining flow parameters.

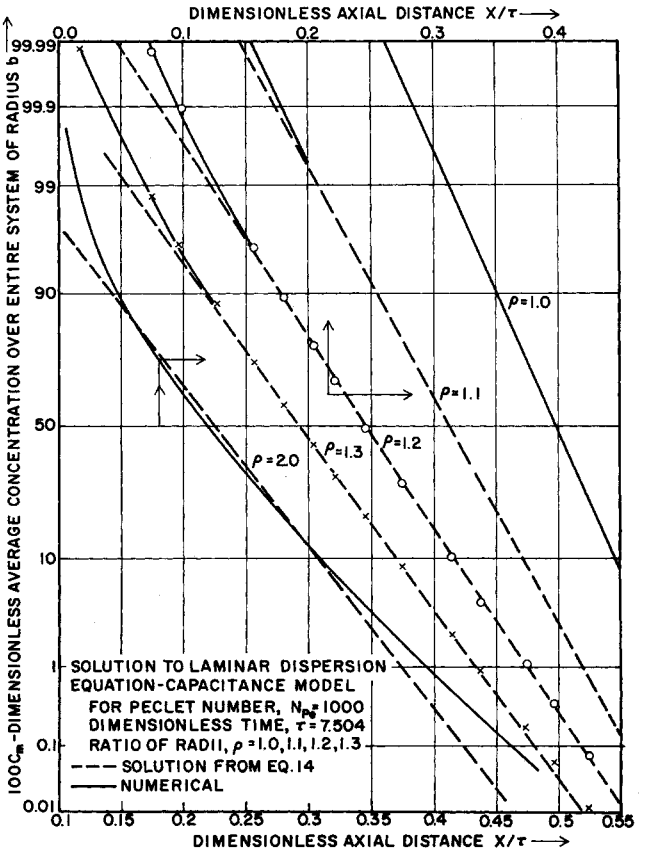

Fig. 7. Comparison of numerical results for different volume ratios in capacitance model with N_{Pe} = 1,000 and dimensionless time τ = 7.504.

Table 2. Comparison of Approximate Analytical Expressions for Different Values of ρ for High Peclet Number Systems

ρ	Argument of error function in Equation (14)	Value of τ above which Equation (14) is valid
1.0	$\left(\frac{X-\tau/2.00}{\sqrt{\tau/48}}\right)$	0.8
1.1	$\left(\frac{X-\tau/2.42}{\sqrt{\tau/31.0}}\right)$	1.25
1.2	$\left(\frac{X-\tau/2.88}{\sqrt{\tau/24.8}}\right)$	2.00
1.3	$\left(\frac{X-\tau/3.38}{\sqrt{\tau/22.3}}\right)$	4.00
2.0	$\left(\frac{X-\tau/8.0}{\sqrt{\tau/16.5}}\right)$	>15.0

It was found that Equation (14) agrees extremely well with the numerical solution for all values of τ above which the behavior is an error function. Thus Equation (14) is an approximate analytical solution to the original dispersion equation for high τ and N_{Pe}. Table 2 shows a comparison of the approximate analytical expressions for the five different ρ values and, more importantly, that the magnitudes of τ, above which Equation (14) is valid, increase rapidly with ρ.

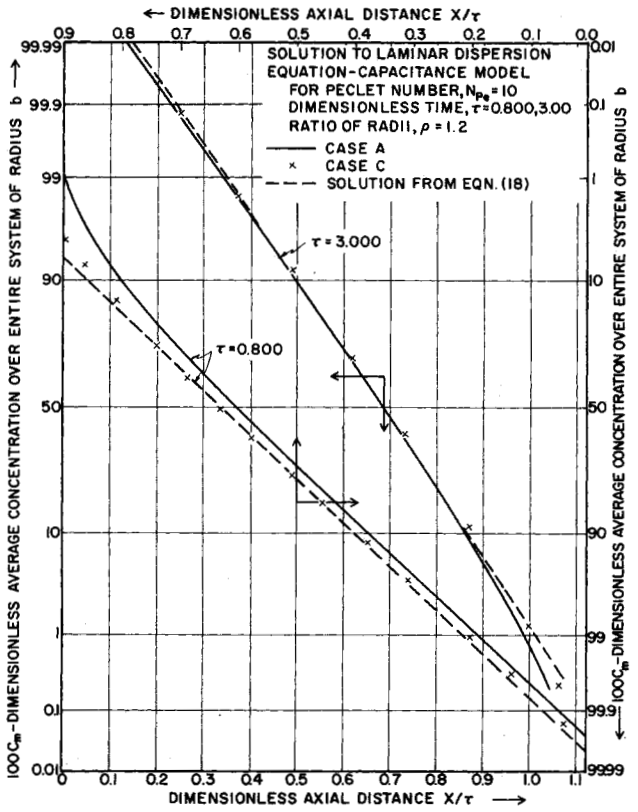

Fig. 9. Comparison of numerical results with Equation (18) for capacitance model with $\rho = 1.2$ and $N_{Pe} = 10$ for two different inlet conditions at dimensionless times $\tau = 0.800$ and 3.000.

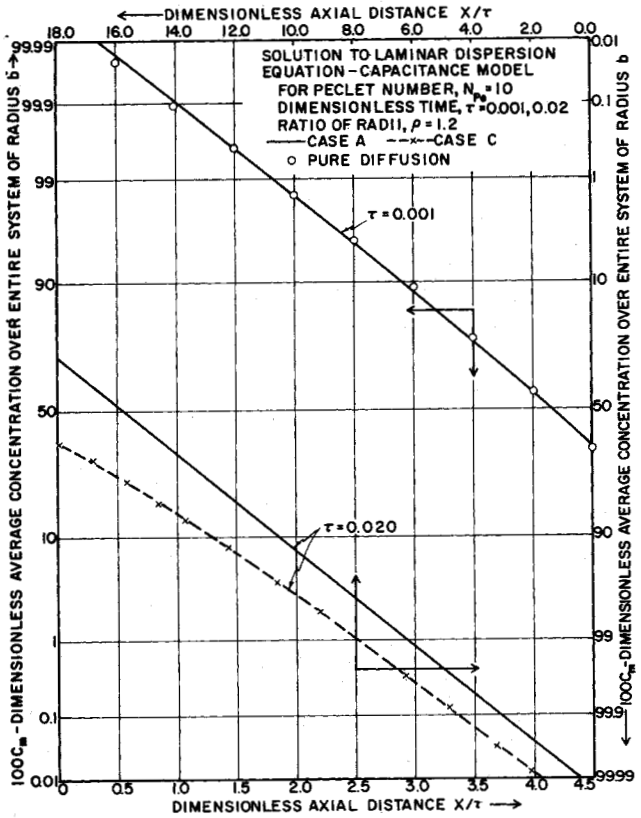

Fig. 8. Comparison of numerical results for capacitance model with $N_{Pe} = 10$ and $\rho = 1.2$. *(a)* Lower curves are for two different inlet conditions at $\tau = 0.020$. *(b)* Upper curve compares pure diffusion solution at $\tau = 0.001$ with numerical results.

The Low Peclet Number Region

As the Peclet number decreases below $N_{Pe} = 100$, axial molecular diffusion becomes a significant transport mechanism. The effect of axial molecular diffusion can be seen clearly in Figures 8 and 9, since the solute extends far beyond $X/\tau = 1.0$. Again, as in the case of simple capillaries, in all these cases it is obvious that the solutions obtained with step change and Danckwerts inlet conditions are different.

At very low Peclet numbers a stage is reached when the dispersion in the main channel takes place essentially by pure diffusion only, as seen in Figure 8. As was done previously with Taylor-Aris diffusion (*1*), it is possible to define the limits for the pure diffusion region in terms of τ and N_{Pe}.* The limits for the pure diffusion region depend on the ratio of the convection to diffusion length, which is proportional to $N_{Pe}\sqrt{\tau}$. Hence, the dispersion occurs by pure diffusion only if the quantity $N_{Pe}\sqrt{\tau}$ is less than a certain value which was found to be approximately

$$N_{Pe}\sqrt{\tau} \begin{cases} < 0.4, & \rho = 1.2 \\ < 0.5, & \rho = 1.0 \end{cases} \qquad (16)$$

As in the case of high Peclet numbers the solutions become linear on probability plots for high τ values. For case A, the higher N_{Pe} the smaller τ must be for the solu-

* The solution to the pure diffusion equation is given in the Appendix.

tions to become error functions, but in cases B and C it is interesting that the time required increases as N_{Pe} is decreased from 1,000 to 25, and then the trend is reversed as the τ required is markedly less at lower N_{Pe}. This is significant, since it shows that the range of applicability of the diffusion model depends on the inlet boundary condition. In particular, on the basis of a step change inlet condition one might mistakenly conclude that the dispersion model is completely impractical for very low N_{Pe} flows, because the dimensionless τ required for it to apply can become so very large. With low values of N_{Pe} an approximate analytical solution can be found by using Aris' modification for the inclusion of axial molecular diffusion. If $\rho = 1.0$, it is known (2) that the approximate solution is given as

$$C_m = 0.5 \operatorname{erfc}\left[\frac{(X-\tau/2)}{\left[\tau/48 + \frac{4\tau}{N_{Pe}^2}\right]^{0.5}}\right] \qquad (17)$$

By applying the same method used in getting a similar expression for high N_{Pe}, the following approximate analytical solution is obtained for low N_{Pe}:

$$C_m = 0.5 \operatorname{erfc}\left[\frac{X-\tau/2\rho^2}{\sqrt{\frac{\alpha\tau}{48\rho^2} + \frac{4\tau}{N_{Pe}^2}}}\right] \qquad (18)$$

Figure 9 shows that the numerical solutions obtained correspond very well with Equation (18) for $\rho > 1.0$ as τ exceeds the minima given in Table 3.

The most significant result given in Table 3 is that the time required in terms of τ for Equation (18) to apply at low N_{Pe} depends markedly on the nature of the inlet boundary conditions in addition to ρ and N_{Pe}. Take $N_{Pe} = 10$ as an example, and it is seen that case A requires an elapsed time three or more times that of cases B and C. This obviously implies that dispersion experiments which employ aperiodic entrance conditions should be designed to simulate case B to reduce the time, and thereby the system length, necessary for the diffusion model to apply.

It is worth noting that ρ appears in Equation (18); consequently, if one views the Turner system as being comparable to a simple capillary of radius b, but characterized by a dispersion coefficient which is increased by the existence of no flow regions, then the dispersion coefficient is α/ρ^2 times that which it would be if pure Poiseuille flow existed throughout the entire system. This suggests that dispersions in complex systems, such as packed beds which exhibit capacitance effects, should be viewed as taking place in the entire void volume; that is, if the flow is laminar and, to a reasonable approximation, is a function of the transverse coordinate only, then not only the dispersion coefficient but, on the basis of results in the next section, also the local concentration distribution can be calculated directly if the parameters which characterize the velocity distribution throughout the entire void volume are known.

TABLE 3. CAPACITANCE MODEL

$\rho = 1.2$; approximate τ values above which:
(i) solution follows Aris' modification for case A
(ii) solution for cases A, B, and C are same
(iii) solution for case B follows Aris' modification

N_{Pe}	τ_{min} for (i)	τ_{min} for (ii)	τ_{min} for (iii)
1,000	2.00	0.0	2.00
25	2.75	0.75	2.75
10	3.50	3.50	1.00
1	>4.00	>4.00	—

Analytical Solution for Local Concentration Distribution

In preceding sections analytical solutions for mean concentration distributions, asymptotic in time, were discussed and shown to be accurate, providing the magnitude of τ was sufficiently large. This section considers a more detailed description of the concentration field in terms of local values. By doing so one can codify and generalize the asymptotic results given previously and also show that this approach yields a remarkably simple and accurate detailed description of local transient behavior in Turner structures. In the following treatment axial molecular diffusion is taken into account.

As suggested by Taylor's analysis for simple tubes, let

$$C = C_m + \frac{\partial C_m}{\partial x_1} f(r) \qquad (19)$$

where $x_1 = x - u_m t$, and the first part of the problem is to find the function $f(r)$. If to a good approximation $(\partial C_m/\partial x_1)$ is constant, then by substituting Equation (19) into Equation (1), one gets

$$u - u_m = D\frac{1}{r}\frac{d}{dr}r\frac{df}{dr} \qquad (20)$$

where

$$\left.\begin{aligned} u &= u_o\left(1-\frac{r^2}{a^2}\right), \quad o \le r \le a \\ u &= o \qquad\qquad , \quad a \le r \le b \end{aligned}\right\} \qquad (21)$$

Integrating Equation (20) twice, one obtains the following expressions for $f(r)$:

$$f(r) = \begin{cases} = f(0) + \frac{1}{D}\left[u_o\left(\frac{r^2}{4} - \frac{r^4}{16a^2}\right) - u_m\frac{r^2}{4}\right], & o \le r \le a \\ = f(0) + \frac{1}{D}\left[\frac{3u_o a^2}{16} + \frac{u_o a^2}{4}\ln\frac{r}{a} - \frac{u_m r^2}{4}\right], & a \le r \le b \end{cases} \qquad (22)$$

In order to evaluate $f(0)$, one has the condition

$$\int_o^b r f(r)\, dr = 0 \qquad (23)$$

and carrying out these integrations with the appropriate expressions given in Equation (22) for $f(r)$, we get

$$f(0) = \frac{u_m b^2}{8D}\left[1 - 4\left(\frac{1}{6\rho^2} + \frac{1}{4} + \ln\rho\right)\right] \qquad (24)$$

With $f(r)$ known, it now remains to determine C_m and this is easily accomplished by multiplying Equation (1) by r and then integrating with respect to r from 0 to b, which yields

$$\frac{\partial C_m}{\partial t} + \frac{2}{b^2}\frac{\partial}{\partial x}\int_o^b urC\, dr = D\frac{\partial^2 C_m}{\partial x^2} \qquad (25)$$

When one substitutes Equation (19) into Equation (25), the result is

$$\frac{\partial C_m}{\partial t} = \left[D - \frac{2}{b^2}\int_o^b urf\, dr\right]\frac{\partial^2 C_m}{\partial x_1^2} = K_1\frac{\partial^2 C_m}{\partial x_1^2} \qquad (26)$$

and from inspection of Equation (26) the dispersion coefficient is clearly

$$K_1 = D - \frac{2}{\rho^2}\int_o^\rho u\, y f(y)\, dy \qquad (27)$$

For Turner structures Equation (27) gives

$$K_1 = D + \frac{a^2 u_o^2}{192D}\left[\frac{8 - 7(1+\beta) + 12(1+\beta)\ln(1+\beta)}{(1+\beta)^2}\right] \qquad (28)$$

and if one notes that

$$C_m = 0.5\ \text{erfc}\left[\frac{x - u_m t}{\sqrt{4K_1 t}}\right]$$

it is clear that α, as employed in Equation (18), would be equal to

$$\alpha = \frac{8(1+\beta) + 12(1+\beta)^2\ln(1+\beta) - 7(1+\beta)^2}{(1+\beta)^2} \qquad (29)$$

This is exactly identical to the result obtained by Aris, who used the method of moments (5). If one expands the logarithm in Equation (29) and collects terms, the result is

$$\alpha = \frac{1 + 6\beta + 11\beta^2 + 4\beta^3 - \beta^4 + \ldots}{(1+\beta)^2} \qquad (30)$$

Clearly, the first three terms of the numerator of Equation (30) are identical to Aris' formula for rectangular pockets (4). These two results yield identical values for α if $\rho = 1.0$ and for the cases studied here, the rectilinear approximation [Equation (30)] of annular type pockets [Equation (29)] differed by about 10% at $\rho = 1.3$. By substituting Equations (18), (22), and (24) into Equation (19) and by transforming into dimensionless quantities, the following expressions are obtained:

$$C = C_m - \frac{1}{4\sqrt{K\pi}}\exp\left[-\frac{(X - \tau/2\rho^2)^2}{K}\right]\left\{\left(1 - \frac{1}{2\rho^2}\right)y^2 - \frac{y^4}{4} - \left[\frac{1}{6\rho^2} + \ln\rho\right]\right\} \qquad (31)$$

for $0 \leq y \leq 1$, and

$$C = C_m - \frac{1}{4\sqrt{K\pi}}\exp\left[-\frac{(X - \tau/2\rho^2)^2}{K}\right]\left\{\ln y - \frac{1}{2\rho^2}y^2 - \left[\frac{1}{6\rho^2} + \ln\rho - \frac{3}{4}\right]\right\} \qquad (32)$$

for $1 \leq y \leq \rho$, where

$$K = \frac{\alpha\tau}{48\rho^2} + \frac{4\tau}{N_{Pe}^2} = (\tau/\rho^2)\left[\frac{\alpha}{48} + \frac{4\rho^2}{N_{Pe}^2}\right] \qquad (33)$$

and C_m is given by Equation (18).

In Figure 10 the numerical solution is compared with the solution obtained from Equations (31) and (32), and in two of the typical cases shown there is good agreement between the results. It was found that the solutions for local concentration distributions given by Equations (31) and (32) and those obtained numerically agree very well in all cases where τ is sufficiently large for Equation (26) to be valid as given in Table 3. This is a remarkably simple result and it is important because it suggests that local as well as average behavior of complex systems can be described accurately by the dispersion model if only the local velocity distribution is known.

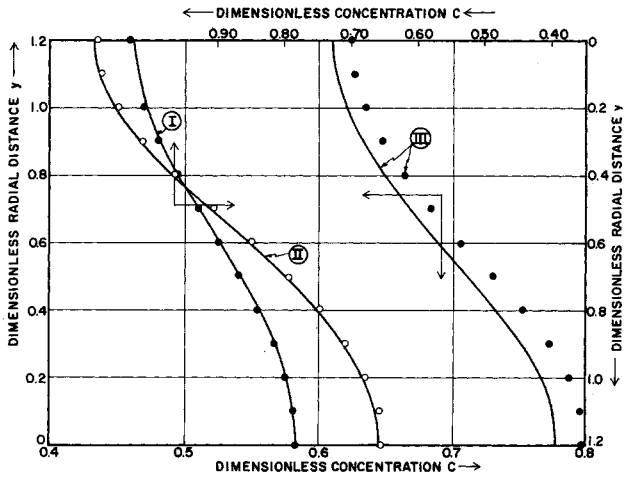

Fig. 10. Comparison of numerical results with approximate analytical solution for local concentration distributions for capacitance model with ρ = 1.2 and N_{Pe} equal 1,000 and 25. Curve I: N_{Pe} = 25, τ = 5.0, X = 1.735, ● = numerical solution, —— = solution from Equations (31), (32), and (33). Curve II: N_{Pe} = 1,000, τ = 2.00, X = 0.69. ○ = numerical solution. —— = solution from Equations (31), (32), and (33). Curve III: N_{Pe} = 1,000, dimensionless time τ = 0.800, axial distance X = 0.2775. ● = numerical solution. —— = solution from Equations (31), (32), and (33).

In order for longitudinal molecular diffusion in the main channel to be negligible, it is necessary that $D << \alpha \frac{b^2 u_m^2}{D}$, which yields

$$N_{Pe} >> \frac{2\rho}{\sqrt{\alpha}}$$

and with $\rho = 1.2$ this yields $N_{Pe} >> 10$, whereas for $\rho = 1$ the requirement was $N_{Pe} >> 13.8$. Thus, as the dead space to channel volume ratio increases, the Peclet number below which axial molecular diffusion is important decreases. This occurs because the existence of stagnant pockets enhances axial dispersion, resulting from axial convection and radial diffusion relative to axial molecular diffusion.

CONCLUSIONS

1. The effect of inlet boundary conditions on the transient approach to the asymptotic Taylor-Aris theory was studied for three different cases. It was found that for values of τ of practical interest solutions were different for these cases only if $N_{Pe} < 100$. The solution was independent of inlet conditions once τ exceeded the necessary minima given in Table 1. In the low Peclet number region the Taylor-Aris model was found to apply for significantly greater ranges of τ for case B than for the step change inlet condition, case A.

2. Higher capacitance systems require significantly longer dimensionless times before their dispersion behavior can be described by error functions. This is important since only then is the concept of an equivalent axial dispersion coefficient really useful because it allows the calculation of the complete average concentration distribution from a minimum of data. Thus, work on high capacitance systems, such as packed beds, should be carried out

in systems of sufficient length for the asymptotic theory to apply.

3. Numerical results for the Turner model agree very well with the modified effective dispersion coefficient suggested by Aris and given in Equation (15), as long as τ is sufficiently large. In the low N_{Pe} range, inlet boundary conditions markedly effect the time necessary for the analytical solution to be valid and in case B, Equation (18) is found to hold for much greater τ ranges than it does in case A.

4. Rather complete numerical solutions to the equation describing laminar dispersion in Turner structures with continuous stagnant pockets of arbitrary depth have been obtained, and results for point, average, and bulk concentration distributions are presented for a wide range of parameters. The range of results covered is extended to essentially all values of τ and N_{Pe} by Equations (31) and (32), which were developed in the present study.

When the lower limits of τ given in Table 3 are exceeded, Equations (31) and (32) are valid for all values of N_{Pe}, since it is not necessary to assume that axial molecular diffusion is negligible. This suggests that expressions which describe the detailed local behavior of complex laminar systems can be determined in a remarkably simple fashion if the velocity distribution throughout the entire system can be approximated reasonably well by a function of the transverse coordinate only. It would seem that this aspect of the present work should be investigated further for systems of more general geometry and multiple streams of different physical properties.

ACKNOWLEDGMENT

This work was supported in part by the Office of Saline Water, U.S. Department of Interior. The numerical calculations were supported by NSF Grant GR-1137 to the Syracuse University Computing Center.

NOTATON

a = radius of main channel
b = radius of whole tube including stagnant pocket
C^+ = concentration of solute at $x = 0$
C^+_∞ = concentration of solute at $x = -\infty$
C = dimensionless concentration C^+/C^+_∞
C_m = dimensionless average concentration, C^+_m/C^+_∞
C_{bulk} = dimensionless bulk concentration
D = molecular diffusion coefficient
i = subscript denoting the interval in the η direction
j = subscript denoting the interval in the y direction
k = effective axial diffusivity
K = $(\alpha\tau/48\,\rho^2) + (4\tau/N_{Pe}^2)$, see Equation (32)
M = total number of intervals in η direction
N = total number of intervals in y direction
n = subscript denoting interval in the τ direction
N_{Pe} = Peclet number, au_o/D
r = radial distance
t = time
$u(y)$ = velocity in axial direction
u_o = maximum velocity at center of the tube
u_m = average velocity $(u_o/2)\,(a/b)^2$
x = axial distance along the tube
X = dimensionless axial coordinate $(Dx/a^2\,u_o)$
x_1 = axial distance relative to axes which move with mean flow; $x - 1/2\,u_m\,t$
y = dimensionless radial coordinate r/a

Greek Letters

α = ratio of dispersion coefficient in Turner model to that in tube
η = dimensionless axial coordinate $X/\sqrt{\tau}$
τ = dimensionless time Dt/a^2
ρ = ratio of radii b/a
η_1 = axial coordinate $XN_{Pe}/2\sqrt{\tau}$
β = total volume of stagnant pocket per unit volume of channel $(\rho^2 - 1)$

LITERATURE CITED

1. Ananthakrishnan, V., W. N. Gill, and A. J. Barduhn, *A.I.Ch.E. J.*, **11**, 1063 (1965).
2. Aris, Rutherford, *Proc. Roy. Soc.*, **235A**, 67 (1956).
3. ———, *Chem. Eng. Sci.*, **10**, 80 (1959).
4. *Ibid.*, **11**, 194 (1959).
5. ———, *Proc. Roy. Soc.*, **252A**, 538 (1959).
6. Peaceman, D. W., and H. H. Rachford, *J. Soc. Ind. Appl. Math.*, **3**, 28 (1955).
7. Philip, J. R., *Australian J. Phys.*, **16**, 287-299 (1963).
8. Taylor, G. I., *Proc. Roy. Soc.*, **219A**, 186 (1953).
9. Turner, G. A., *Chem. Eng. Sci.*, **7**, 156 (1958).
10. *Ibid.*, **10**, 14 (1959).
11. Wehner, J. F., and R. H. Wilhelm, *ibid.*, **6**, 89 (1956).

APPENDIX

At sufficiently small values of N_{Pe} the dispersion equation with no convection describes the capacitance model. On averaging the equation, the y dependent terms vanish and the resulting equation is

$$\frac{\partial C_m}{\partial \tau} = \frac{1}{N_{Pe}^2}\,\frac{\partial^2 C_m}{\partial X^2} \tag{A1}$$

One must consider Equation (A1) together with initial conditions given by

$$\left.\begin{aligned} C_m(0, X) &= 0 \\ C_m(\tau, 0) &= f(\tau) \end{aligned}\right\} \tag{A2}$$

where $f(\tau)$ is some function of τ which is unknown as yet. From the numerical results obtained for case A and $\rho = 1.2$, an approximate expression for $f(\tau)$, valid for τ values ≤ 0.5, was found to be given by

$$f(\tau) = 0.555\sqrt{\tau} + 0.632 \tag{A3}$$

By using this function and by applying Duhamel's theorem, the solution to the pure diffusion equation is obtained as

$$C_m = 0.555\sqrt{\pi\tau}\left[\frac{1}{\sqrt{\pi}}\,e^{-\eta_1^2} - \eta_1 \operatorname{erfc}\eta_1\right] + 0.632\operatorname{erfc}\eta_1 \tag{A4}$$

where $\eta_1 = XN_{Pe}/2\sqrt{\tau}$. It is clearly seen that Equation (A4) satisfies Equation (A1) and the initial and boundary conditions given by Equation (A2).

The limits for the pure diffusion region depend on the ratio of the convection to the diffusion length which is proportional to $N_{Pe}\sqrt{\tau}$. Hence the dispersion occurs essentially by pure diffusion if the quantity $N_{Pe}\sqrt{\tau}$ is less than a certain value A. This value of A was determined by plotting N_{Pe} vs. the value of τ below which the pure diffusion solution holds to within about 2% or less. It was found that this plot is linear on logarithmic scales and from the slope and the intercept, the value of A is found to be approximately equal to 0.4. Hence the requirement for the pure diffusion Equation (A4) to hold can be written as

$$N_{Pe}\sqrt{\tau} < 0.4 \tag{A5}$$

Manuscript received November 1, 1965; revision received March 18, 1966; paper accepted March 30, 1966. Paper presented at A.I.Ch.E. Dallas meeting.